J. Fluid Mech. (1987), *vol.* 177, *pp.* 359–379
Printed in Great Britain

The response of a stratified rapidly rotating flow to a pulsating topography

By S. N. BROWN
Department of Mathematics, University College London WC1E 6BT, UK

AND H. K. CHENG
Department of Aerospace Engineering, University of Southern California, Los Angeles, CA 90089-0192, USA

(Received 4 November 1985 and in revised form 5 May 1986)

A theoretical study is made of the disturbance produced by an oscillating, shallow topographical feature in horizontal relative motion in a rapidly rotating, linearly stratified, unbounded fluid. For a sinusoidal surface oscillation, an explicit solution is obtained in terms of wavenumber spectra of the topography. The oscillating far-field behaviour is shown to consist of a large-scale, cyclonic component above the topography and a system of inertial waves behind the caustics, which spreads predominantly in the downstream direction. A significant property of the flow field is its dependence on a frequency threshold familiar from classical works on internal gravity waves in the absence of rotation, determined by the Brunt–Väisälä value. When the frequency is supercritical, a prominent circle of maximum disturbance appears in the far field, which provides the transition boundary between two distinct cyclonic structures and an upstream barrier to the propagating waves ahead of the obstacle. The circle has a radius depending on the relative magnitude of the pulsating frequency and the Brunt–Väisälä value, and is distinctly marked also by a phase jump in pressure and velocities. These features are substantiated by numerical examples of the full solution at a large but finite distance above the obstacle at supercritical frequencies. The circle of maximum disturbance signifies a preferential direction for energy propagation unaccounted for by group velocity. Its relation to the classical result of Görtler in the homogeneous case and that in the classical internal-gravity-wave theory are examined.

1. Introduction

The effects of topography on the flow field in rotating and stratified fluids are important aspects of both meteorology and oceanography. These effects will be studied in the context of a deep, rapidly rotating fluid. Many important concepts of geophysical fluid dynamics and their applications are concerned with quasi-geostrophic, hence rapidly rotating, fluid motion (Batchelor 1967; Pedlosky 1979; Yih 1965, 1980). This calls for a small Rossby number $\mathscr{R} \equiv u_c/\Omega_c L$, where u_c and L are a typical relative velocity and typical horizontal scale, respectively, and Ω_c is the constant angular speed of the rotating fluid. The following analysis represents therefore an aspect of the asymptotic theory of low $\mathscr{R}$ flow. Of interest to the theoretical development are those topographical and flow configurations which can be modelled in laboratory experiments, so the problem will be formulated for obstacles with simple geometry in steady horizontal motion on the base of a deep

container that is rotating about a vertical axis, as in the experiments of Hide, Ibbetson & Lighthill (1968), Maxworthy (1977), and Heikes & Maxworthy (1982). The use of a deep container is important, since topographical features with scales small compared to the height or depth of the atmosphere or ocean are also of geophysical relevance. The cited laboratory studies call attention to departures from the familiar Taylor-column description at large distances from the obstacle, for which an inertial correction to the geostrophic balance, though small, is crucial. Both theoretical and experimental studies (Lighthill 1967; Hide *et al.* 1968) suggest a slight tilt of an order $\mathscr{R}$ in the columnar structure towards downstream, although the observed flow patterns are expected to be greatly influenced by the fluid viscosity in these experiments (see analyses in Mason & Sykes 1979; Johnson 1982, and discussion in Stewartson & Cheng 1979).

1.1. *Inertial-wave patterns in a deep container*

Considering an obstacle in steady motion as a source of outgoing inertial waves, Lighthill (1967, 1978) has successfully applied the group-velocity/stationary-phase method (Lighthill 1965; Whitham 1973) to the far-field analysis for both rotating and stratified flows. Cheng (1977) derived formally the equations for nonlinear inertial waves for a homogeneous fluid in a deep container as an outer problem for $\mathscr{R} \ll 1$, and solved the linearized boundary-value problem for an arbitrary shallow topography. Cheng's solution confirms most features noted in Lighthill's (1967) analysis, except that his lee-wave amplitude does not attenuate far downstream as required in Lighthill's concept of tilting. The discrepancy (resulting from an omission of a constant in the stationary phase) was subsequently resolved in Cheng & Johnson (1982) where the far-field structure is also shown to depend strongly on the topographical details. The pronounced influence of the container depth was studied in Stewartson & Cheng (1979), which brings out a columnar, depth-dependent structure in addition to the quasi-random, persistent character of the lee-wave pattern resulting from wall reflection. The analysis shows that the effect of the depth H is controlled by $\mathscr{R}H/L$, irrespective of the obstacle thickness, which explains the persistent lee-wave patterns observed in Maxworthy's (1977) laboratory study.

1.2. *Stratification and the cyclonic disturbance*

An important result brought out in Lighthill's (1967) study is the wedge-shaped caustic front, downstream of which the inertial waves are confined; the leading edge of this wedge is a vertical rising from the obstacle parallel to the rotation axis. Extending Lighthill's group-velocity method, Redekopp (1975) considered the problem for a linear stratification in a rotating fluid, and found that the stratification effect is to tilt the leading edge of the caustic from the vertical towards downstream, with a tilting angle proportional to the Brunt–Väisälä frequency (even though the caustic surface itself is no longer of a wedge shape). This discovery thus furnishes a tilting angle more distinct than that in Lighthill's (1967) homogeneous-fluid model. On the other hand, the result suggests that the disturbances would be swept out of sight along with the caustic when the stratification is high – a conclusion at variance with existing analyses which model the topographical problem in a strongly stratified and rapidly rotating fluid (Hogg 1973, 1978; Ingersoll 1969; Huppert 1975; Buzzi & Tibaldi 1977; Johnson 1978; Smith 1979*a*, *b*). This paradox was addressed in Cheng, Hefazi & Brown (1984), which is hereinafter referred to as I and may be regarded as an extension of Cheng & Johnson (1982) to a linearly stratified rotating fluid. The solution to the boundary-value problem obtained therein reveals, in

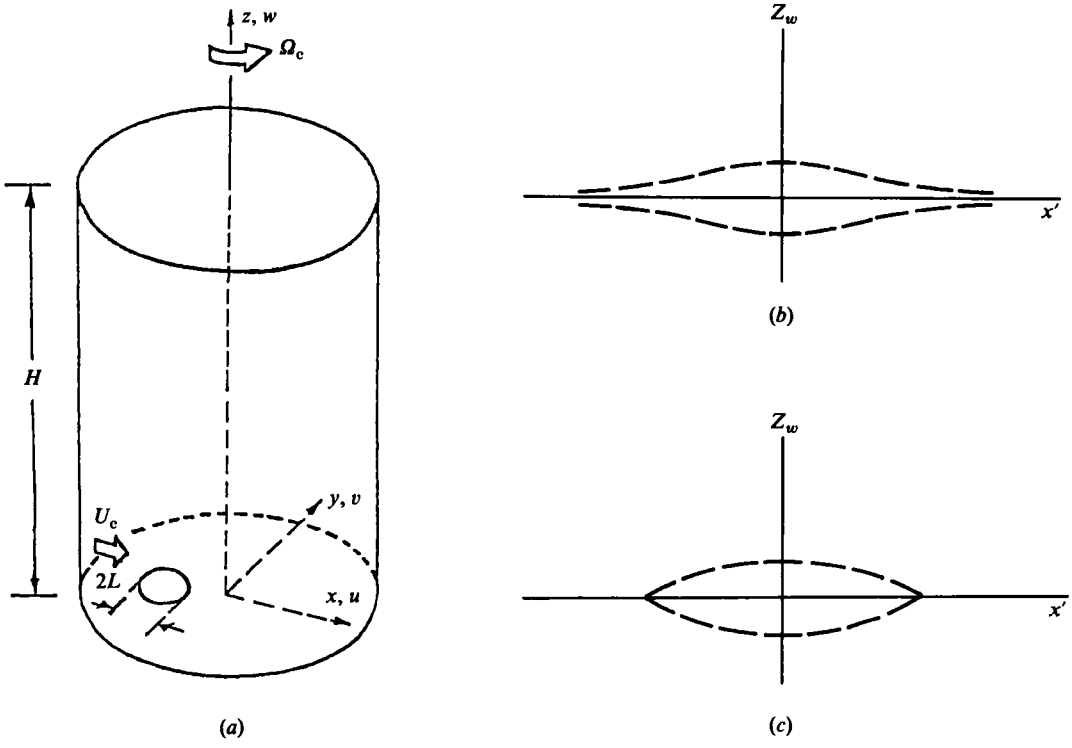

FIGURE 1. (*a*) Illustration of coordinates and notation used in the analysis. Typical profiles of the obstacle/topography considered are sketched in (*b*) and (*c*) with dashes indicating the envelope of the periodic surface motions.

addition to the inertial-wave pattern, the presence of a large-scale, non-wavy, cyclonic disturbance for all but the homogeneous case. This cyclonic feature should not be too surprising at least for a strong stratification, since the horizontal stream function can be identified with the solution to a Neumann problem of the Laplace equation in this case, to which the governing equations in a certain limit corresponding to an infinite stratification reduce. This feature may be interpreted as having resulted from the very long waves close to the zero wavenumber, which is a singularity in the dispersion relation of the present problem, and hence was precluded by the group-velocity or saddle-point method, but may nevertheless be treated as an end-point contribution. The work of I is concerned with a uniform relative motion, and it is not at all clear how an unsteady motion, and a sinusoidally oscillating topography in particular, may affect the occurrence and the structure of the cyclonic disturbance.

1.3. *Periodically pulsating topography*

The present paper extends the results of I to the situation in which the moving obstacle corresponding to the topographical feature has, in addition to its uniform translation, a heaving motion in a single Fourier mode. As in I, we assume a Boussinesq fluid, consider a slow translation ($\mathscr{R} \to 0$) and a vanishingly small heaving amplitude ($\tau \to 0$), and shall examine the combined effect of the heaving undulation and stratification. A problem typical of those analysed is illustrated in the sketch in figure 1.

While the present analysis is limited to a single sinusoidal temporal mode, the result provides detailed knowledge of the flow response to any Fourier component in the frequency spectrum of an arbitrary unsteady movement of a shallow topography. Of interest is the response in the high- and low-frequency ranges, which should indicate, for instance, how rapidly or slowly the cyclonic and related features may evolve in a transient problem. With a suitable integration path, the solution to an initial-value problem may also be constructed by inverting the Fourier transform which is in fact proportional to the frequency response analysed here; this however is not the objective of the present paper. An alternative to the present analysis is to consider an approach by which the solution to a more general initial boundary-value problem can be constructed via the Duhamel integral; this has been undertaken by Hefazi (1985, and also in unpublished work by H. Hefazi & H. K. Cheng 1986) and applied to a study of the evolution processes of the anticyclonic and cyclonic patterns above and downstream of a compact topography, respectively. Certain outstanding features of the evolutionary solution numerically obtained therein can be explained by the results obtained below. The present analysis will also bring out several interesting features of periodic motion, not readily apparent from an initial-value approach; the two approaches are thus complementary.

1.4. *Remarks on content*

In §2, we set out the relevant linearized equations for the shallow pulsating topography and proceed to construct the solution from propagating wavetrains after a careful selection of the proper branches from the dispersion relation. The resulting solution admitted by the boundary-value problem consists of two families of wavetrains as in I: one is made up of outgoing wavetrains with a non-attenuating upward-propagating component and the other is composed of the evanescent wavetrains which attenuate in the upward direction. By virtue of their exponentially high attenuation rate, evanescent wavetrains contribute little to the far field, except for long wavetrains corresponding to the zero wavenumber which may fall in the evanescent-wave range in some cases (as in I). The wavenumber origin corresponding to those very long waves remains a singularity of the dispersion relation for all frequencies; its contribution to the far field has to be specially treated. Section 3 delineates the major far-field features of the inertial waves belonging to the outgoing wave family, using the stationary-phase method, and also including a novel way of deducing the shapes of the caustic surfaces. The contribution of the singularity at the wavenumber origin unaccounted for by the stationary-phase method is treated in §4, where frequency-dependent, far-field disturbances in cyclonic form are brought out. Of significance are the major changes from a subcritical far-field behaviour when the forcing frequency Ω exceeds the Brunt–Väisälä value N, familiar from the classical work on internal gravity waves without background rotation (Yih 1980, pp. 60–67). Particularly prominent when this frequency threshold is exceeded ($\Omega > N$) is an upwardly extended conical surface which spatially divides two distinct cyclonic structures, and is also a caustic boundary for propagating waves ahead of the obstacle. Both analyses in §§3 and 4 become singular at the conical surface, and a transitional solution valid in the vicinity of this boundary is presented in §5 where the magnitude of the maximum far-field disturbance is established. The findings are substantiated by a numerical evaluation of the full solution for two supercritical examples; the anticipated features are clearly visible at large but finite scaled heights.

In passing, we recall that the presence of inertial waves ahead of the obstacle in an unsteady case has been noted in Redekopp's (1975) study. Its critical dependence

on a frequency threshold and the existence of the circle of maximum amplitude were not brought out. An apparently similar, but not identical, frequency threshold for the inertial-wave pattern is quite well known in rotating-fluid theory for the *homogeneous* case (Görtler 1944; see Greenspan 1968, p. 10, and plate 8; Yih 1980, p. 331) in that, when the forcing frequency Ω falls *below* twice that of the rotating container, $2\Omega_c$, a conical characteristic surface emanating from the oscillating source emerges. The two critical frequencies $\Omega = 2\Omega_c$ and $\Omega = N$ may very well represent the upper and lower limits for the existence of circular caustics, even though the threshold $\Omega = N$ found below is a result pertaining mainly to the geostrophic limit $\mathscr{R} \to 0$ (cf. discussion in §7).

2. The geometry and the equations of motion for a thin obstacle in a container of infinite depth

2.1. *Basic theoretical model*

Except for the oscillatory bottom topography, the geometry of the situation is exactly that of I. We briefly rederive the equations of motion in the limit required here. A stably stratified inviscid fluid confined between the planes $z^* = 0$ and $z^* = H$, and rotating about the vertical axis with constant angular speed Ω_c, has a slow horizontal component of velocity over a topographical feature in the plane $z^* = 0$. Axes $Ox^*y^*z^*$ rotate with the undisturbed fluid and, if the flow is taken to be symmetric about $z^* = 0$, it is equivalent to assuming the presence of an obstacle if we take it as moving from *left* to *right* in the Ox^* direction with uniform speed u_c. A Boussinesq fluid is assumed with a linear density variation ρ_e^* when it is undisturbed in the form

$$\frac{\rho_e^* - \rho_0^*}{\rho_0^*} = -\frac{\epsilon}{H} z^*, \tag{2.1}$$

with ρ_0^* the density at $z^* = 0$, ϵ being a positive constant. The stratification parameter is again as in I, namely

$$\theta \equiv \frac{g\epsilon L^2}{H u_c^2} = \left(\frac{NL}{u_c}\right)^2, \tag{2.2}$$

where L is the horizontal length of the moving body, g the acceleration due to gravity, and N the Brunt–Väisälä frequency $(g\epsilon/H)^{\frac{1}{2}}$. The present study will be concerned mainly with a positive θ.

2.2. *Reduced equations for an initial boundary-value problem*

We now write $(x^*, y^*, z^*) \equiv L(x, y, \tilde{z}/\mathscr{R})$ and denote the velocities in the corresponding directions by $\tau u_c(u, v, w)$, the time by Lt/u_c, the departure from the equilibrium pressure by $\tau \rho_0^* \Omega_c u_c L_0^* \tilde{p}$ and from the equilibrium density by $\tau \epsilon L \rho_0^* \rho / H$. Here τ is a measure of the maximum amplitude of the pulsating body and $\mathscr{R}$ ($\equiv u_c/\Omega_c L$) the Rossby number. If the equations of motion are non-dimensionalized and it is assumed that both $\tau \ll 1$ and $\mathscr{R} \ll 1$ then the linear system (Cheng 1977; Stewartson & Cheng 1979)

$$\left.\begin{aligned} -2v + \frac{\partial \tilde{p}}{\partial x} = 0, \quad 2u + \frac{\partial \tilde{p}}{\partial y} = 0, \quad \frac{\partial \tilde{p}}{\partial \tilde{z}} + \frac{\partial w}{\partial t} + \theta\rho = 0, \\ 2\frac{\partial w}{\partial \tilde{z}} - \frac{\partial}{\partial t}\left(\frac{\partial v}{\partial x} - \frac{\partial u}{\partial y}\right) = 0, \quad \frac{\partial \rho}{\partial t} - w = 0, \end{aligned}\right\} \tag{2.3}$$

is obtained. The boundary condition on the moving obstacle whose equation is $\tilde{z} = Z_w(x-t, y, t)$ may be transferred to the plane $\tilde{z} = 0$ as

$$w = \frac{\partial}{\partial t} Z_w(x-t, y, t) \quad \text{on } \tilde{z} = 0. \tag{2.4}$$

Upon setting

$$x' = x-t, \quad \hat{z} = \tfrac{1}{2}\tilde{z}, \quad \psi = -\tfrac{1}{2}\tilde{p} \tag{2.5}$$

we recover the equation

$$\left\{\frac{\partial^2}{\partial \hat{z}^2} + \left[\left(\frac{\partial}{\partial t} - \frac{\partial}{\partial x'}\right)^2 + \theta\right]\left(\frac{\partial^2}{\partial x'^2} + \frac{\partial^2}{\partial y^2}\right)\right\}\psi = 0, \tag{2.6}$$

with

$$\frac{\partial \psi}{\partial \hat{z}} - \left[\left(\frac{\partial}{\partial t} - \frac{\partial}{\partial x'}\right)^2 + \theta\right] Z_w(x', y, t) = 0 \quad \text{at } \hat{z} = 0, \tag{2.7}$$

exactly as in I. The coordinates $(x', y, \hat{z})$ move with the body, and in order to obtain (2.6) and (2.7) an operator $\partial/\partial t$ on the left-hand side of each equation has been suppressed on the assumption that (2.6) and (2.7) hold at $t = 0$. We shall now take $\mathscr{R}H/L$ to be infinite and replace the boundary condition on the upper plane by the requirement that $\psi \to 0$ as $x'^2 + y^2 + \tilde{z}^2 \to \infty$ and that there are only outgoing waves in the far field. To complete the problem formulation, appropriate initial condition data (e.g. initial data of ψ and $\partial\psi/\partial t$) must be prescribed, which are unnecessary in the following analysis of the frequency response.

2.3. *The frequency response: solution to a boundary-value problem*

In addition to its motion from left to right, we shall assume that the body is also heaving in a single Fourier mode so that

$$Z_w(x', y, t) = \overline{Z}_w(x', y)\, \mathrm{e}^{\mathrm{i}pt}, \quad p > 0, \tag{2.8}$$

where the real part of the final result is to be taken. Note that p is related to the physical radian frequency Ω by $p = \mathscr{R}^{-1}\Omega/\Omega_c$.

The solution of (2.6) subject to (2.7) may be written down at once in the form $\psi = \overline{\psi}\, \mathrm{e}^{\mathrm{i}pt}$ with

$$\overline{\psi} = \int_{-\infty}^{\infty}\int_{-\infty}^{\infty} h(\omega, \sigma) \exp\{\mathrm{i}[\omega x' + \sigma y + ((\omega-p)^2 - \theta)^{\frac{1}{2}}\, (\omega^2+\sigma^2)^{\frac{1}{2}}\hat{z}]\}\, \mathrm{d}\omega\, \mathrm{d}\sigma, \tag{2.9}$$

where

$$h(\omega, \sigma) = \mathrm{i}(2\pi)^2 F(\omega, \sigma)((\omega-p)^2 - \theta)^{\frac{1}{2}}\, (\omega^2+\sigma^2)^{-\frac{1}{2}}, \tag{2.10}$$

and $F(\omega, \sigma)$ is the double Fourier transform of $\overline{Z}_w(x', y)$ so that

$$F(\omega, \sigma) = \int_{-\infty}^{\infty}\int_{-\infty}^{\infty} \overline{Z}_w(x', y)\, \mathrm{e}^{-\mathrm{i}\omega x' - \mathrm{i}\sigma y}\, \mathrm{d}x'\, \mathrm{d}y. \tag{2.11}$$

In (2.9) and (2.10), $(\omega^2+\sigma^2)^{\frac{1}{2}}$ is the positive square root of the positive quantity, and the sign of $((\omega-p)^2-\theta)^{\frac{1}{2}}$ is to be chosen so that $\overline{\psi}$ remains bounded as $\hat{z} \to \infty$, and so that there are only *outgoing waves* for $\hat{z} \gg 1$. Two ways of looking at this, which both lead to the same result when $p = 0$, are either to consider the present problem as the long-time limit of an initial-value problem with Laplace transform parameter s or to use group-velocity arguments. With $p \neq 0$ we may either choose the correct

root with s real and positive and set $s = \mathrm{i}p$ on completion, or we may simply choose the root which reduces to that of I as $p \to 0$. In either case we obtain

$$((\omega-p)^2-\theta)^{\frac{1}{2}} = \pm|(\omega-p)^2-\theta|^{\frac{1}{2}} \quad \text{if } \omega-p > \theta^{\frac{1}{2}},$$

$$\text{or } \omega-p < -\theta^{\frac{1}{2}}, \quad \text{when } |\omega-p| > \theta^{\frac{1}{2}}; \quad (2.12a)$$

$$((\omega-p)^2-\theta)^{\frac{1}{2}} = \mathrm{i}|(\omega-p)^2-\theta|^{\frac{1}{2}}, \quad \text{when } |(\omega-p| < \theta^{\frac{1}{2}} \quad (2.12b)$$

The ranges of ω in (2.12a) give an oscillatory contribution to (2.9) which represents the outgoing inertial waves, while those in (2.12b) give a contribution to the integral that decays exponentially with $\hat{z}$. We note that in the case of a finite depth ($\mathscr{R}H/L \neq \infty$), other roots of the dispersion relation, including exponentially growing components must be allowed to account adequately for the reflection from the upper boundary.†

2.4. *Preliminary remarks on the far-field analysis: anticipated results*

In the following sections we discuss the far-field asymptotics of $\overline{\psi}$ in (2.9) by examining the leading terms of its asymptotic expansion for large $\hat{z}$. The integral (2.9) for large $\hat{z}$ has contributions not only from the stationary phase but also from the wavenumber origin, where the phase is singular and which must be separately treated. These two types of contribution are analysed in §§3 and 4 where special attention will be paid to the critical changes in the far-field structure brought about by the relative magnitude of p and $\theta^{\frac{1}{2}}$. The far-field study is completed in §5 where the non-uniformity of the results in §§3 and 4 at the circular boundary in the supercritical case is treated and the magnitude of the maximum disturbance is established.

We shall find that the dominant contributions come from the saddle points for $|\omega-p| > \theta^{\frac{1}{2}}$, for those values of $x'/\hat{z}$, $y/\hat{z}$ for which they exist, and from the origin $\sigma = 0 = \omega$. With the saddle points is associated a caustic within which the resulting lee waves are confined, while the singularity at the origin gives rise to a cyclonic disturbance comparable with, but clearly distinguishable from, that noted in I. The lee waves decay as $\hat{z}^{-1}$ except in the neighbourhood of the caustic where the decay rises to $O(\hat{z}^{-\frac{1}{3}})$. The situation $p < \theta^{\frac{1}{2}}$ is very like that of I (corresponding to $p = 0$) except that now the caustic curve has two branches (though it is unlikely that they could be differentiated in a numerical evaluation of (2.9) for finite $\hat{z}$). When $p > \theta^{\frac{1}{2}}$ it emerges that the lee waves are present ahead of the obstacle, specifically in a circle of radius proportional to $(p^2-\theta)^{\frac{1}{2}}\hat{z}$, in the neighbourhood of which the decay is $O(\hat{z}^{-\frac{3}{4}})$, except for two symmetrically placed points near which the disturbance increases to $O(\hat{z}^{-\frac{2}{3}})$. The reason for the occurrence of this additional feature of interest is the coincidence of the wavenumber origin and a saddle point that can occur when $p > \theta^{\frac{1}{2}}$ as may be seen from (2.12a).

The anticipated results in §§3, 4 and 5 clearly establish the significance of the critical condition $p = \theta^{\frac{1}{2}}$, which can be written more explicitly as the frequency threshold: $\Omega = N$, independent of Ω_c and $\mathscr{R}$.

† As in most existing theories of hydrodynamic instability, the assumption of a bounded $\overline{\psi}$ at $\hat{z} \to \infty$ does not preclude the possibility of a spatial instability in the downstream (x') direction.

3. The saddle-point contributions to the far field

3.1. *Identification of physical domains of inertial waves*

It was found in I that with $p = 0$ the integrand of (2.9) has four real pairs of values of ω, σ for which the function $\omega\tilde{X}+\sigma\tilde{Y}+(\omega^2-\theta)^{\frac{1}{2}}(\omega^2+\sigma^2)^{\frac{1}{2}}$ is stationary, in a certain region of the $(\tilde{X}, \tilde{Y})$-plane. Here $x' = \tilde{X}\hat{z}, y = \tilde{Y}\hat{z}$. When $p = 0$ this region is $8\tilde{Y}^2 < \tilde{X}^2-8\theta, \tilde{X} < 0$, the boundary of which forms a caustic. At large $\hat{z}$, and correspondingly large x', y, all oscillatory disturbances are confined to this region, which in three-dimensional space is bounded by a conical surface with its vertex at the origin. All such disturbances are behind the body and in particular when $\theta = 0$, the homogeneous situation, the resulting pattern for these gravity waves is reminiscent of that of Kelvin ship waves. Inside the caustic the four real values of ω are $\pm\omega_1$, $\pm\omega_2$, and on the caustic $\omega_1 = \omega_2$. With $p \neq 0$ we shall find that the situation is somewhat different. In the $(\tilde{X}, \tilde{Y})$-plane the caustic now has two branches. Inside the inner branch, again for $\tilde{X} < 0$, there are four real values of $\omega-p$ with corresponding σ, two of which are negative and two positive. The two positive values of $\omega-p$ coincide on the inner branch and then become complex. The two negative values remain real until the outer branch is reached. An additional point of interest is that, for values of $p > \theta^{\frac{1}{2}}$, of the two negative values of $\omega-p$ one exists for $\tilde{X} < 0$ inside the circle $\tilde{X}^2+\tilde{Y}^2 = p^2-\theta$ and the other for $\tilde{X} > 0$. This means that for sufficiently large p the pulsating body generates a certain amount of oscillatory upstream influence at large $\hat{z}$.

To examine the saddle points of the integrand of (2.9) we set

$$\overline{\omega} \equiv \frac{\omega}{p}, \quad \overline{\sigma} \equiv \frac{\sigma}{p}, \quad X \equiv \frac{x'}{p\hat{z}}, \quad Y \equiv \frac{y}{p\hat{z}}, \tag{3.1a}$$

$$\overline{\theta} \equiv \frac{\theta}{p^2} = \left(\frac{N}{\overline{\Omega}}\right)^2, \tag{3.1b}$$

and examine the stationary points of the function

$$\Phi(\overline{\omega}, \overline{\sigma}) = \overline{\omega}X+\overline{\sigma}Y+((\overline{\omega}-1)^2-\overline{\theta})^{\frac{1}{2}}(\overline{\omega}^2+\overline{\sigma})^{\frac{1}{2}}, \tag{3.2}$$

where, from (2.12),

$$((\overline{\omega}-1)^2-\theta)^{\frac{1}{2}} = \pm|(\overline{\omega}-1)^2-\overline{\theta}|^{\frac{1}{2}} \quad \text{if } \overline{\omega}-1 > \overline{\theta}^{\frac{1}{2}},$$

$$\text{or } \overline{\omega}-1 < -\overline{\theta}^{\frac{1}{2}}, \quad \text{when } |\overline{\omega}-1| > \overline{\theta}^{\frac{1}{2}}; \tag{3.3a}$$

$$((\overline{\omega}-1)^2-\overline{\theta})^{\frac{1}{2}} = \mathrm{i}|(\overline{\omega}-1)^2-\overline{\theta}|^{\frac{1}{2}}, \quad \text{when } |\overline{\omega}-1| < \overline{\theta}^{\frac{1}{2}}. \tag{3.3b}$$

At the stationary points $\partial\Phi/\partial\overline{\omega} = 0 = \partial\Phi/\partial\overline{\sigma}$ so that, for $\overline{\omega}$, $\overline{\sigma}$ to be real they are in the ranges $|\overline{\omega}-1| > \overline{\theta}^{\frac{1}{2}}$ of (3.3a). From (3.2) we obtain, on differentiating,

$$0 = X+\frac{2\overline{\omega}^3-3\overline{\omega}^2+\overline{\omega}(1-\overline{\theta})+\overline{\sigma}^2(\overline{\omega}-1)}{(\overline{\omega}^2+\overline{\sigma}^2)^{\frac{1}{2}}((\overline{\omega}-1)^2-\overline{\theta})^{\frac{1}{2}}}, \tag{3.4a}$$

$$0 = Y+\frac{\overline{\sigma}((\overline{\omega}-1)^2-\overline{\theta})^{\frac{1}{2}}}{(\overline{\omega}^2+\overline{\sigma}^2)^{\frac{1}{2}}}. \tag{3.4b}$$

If we eliminate $\overline{\sigma}$ from (3.4) and set

$$\overline{\omega} = 1+\lambda, \tag{3.5}$$

we find that λ satisfies the quartic

$$X^2(\lambda^2-\bar{\theta}-Y^2) = (2\lambda^2+2\lambda-\bar{\theta}-Y^2)^2, \tag{3.6}$$

which may be rewritten as

$$4\lambda^4+4\lambda^3+(1-4\overline{Y}^2-X^2)\lambda^2-2\lambda\overline{Y}^2+\overline{Y}^2(\overline{Y}^2+X^2) = 0, \tag{3.7}$$

where

$$\overline{Y} \equiv (Y^2+\bar{\theta})^{\frac{1}{2}} > 0. \tag{3.8}$$

Descartes' rule of signs tells us that (3.7) cannot have more than two positive roots for $\lambda \equiv \bar{\omega}-1$ or more than two negative roots. Indeed from (3.6) we see that all real roots have $|\lambda| > \overline{Y}$. That for (3.7) a caustic exists is indicated by the fact that for sufficiently large X and bounded $\overline{Y}$ there are four real roots, namely

$$\lambda \approx \pm\overline{Y}, \quad \lambda \approx \pm\tfrac{1}{2}X, \tag{3.9}$$

but for sufficiently large $\overline{Y}$ and bounded X the four roots are

$$\lambda \approx \pm\frac{\overline{Y}}{2^{\frac{1}{2}}}-\tfrac{1}{4}\pm\tfrac{1}{2}\mathrm{i}X \tag{3.10}$$

for all combinations of the signs. Thus the oscillatory disturbance will be confined to some region of the $(X, \overline{Y})$-plane for which $\overline{Y}$ is bounded if X is bounded. To find the boundary of the region which contains the oscillatory disturbance we must first find the equation of the caustic.

3.2. *Generating two branches of the caustic*

To find the caustic curve we eliminate λ between (3.7) and the equation obtained by differentiating it with respect to λ. After some algebra we obtain

$$(1+8\overline{Y}^2-X^2)(4\overline{Y}^2+X^2-1)^2 = 3\overline{Y}^2(1+8\overline{Y}^2+5X^2)(8\overline{Y}^2-X^2-5), \tag{3.11}$$

and that on the caustic $\lambda = \lambda_c$ where

$$\frac{\lambda_c^2}{\overline{Y}^2} = \frac{2(\overline{Y}^2+X^2)+1}{4\overline{Y}^2+X^2-1} \tag{3.12a}$$

and

$$\lambda_c = -\frac{4\overline{Y}^2+X^2-1}{8\overline{Y}^2-X^2-5}. \tag{3.12b}$$

The above equations allow a novel way of generating the caustic surface of interest.

We first discuss the curve (3.11) in the case of the homogeneous limit $\bar{\theta} = 0$, and then to obtain the curve for $\bar{\theta} \neq 0$ we rotate the curve for $\bar{\theta} = 0$ around the X-axis to obtain a body of revolution in (X, Y, Z)-space and cut this body with the plane $Z = \bar{\theta}^{\frac{1}{2}}$. This intersection gives the required curve. The advantage of this is that for $\bar{\theta} = 0$ we are able to consider a variable Y that can take the value zero.

The properties of (3.11) with $\bar{\theta} = 0$ and $\overline{Y}^2 = Y^2$ follow easily. If we write it as

$$64\,Y^6+48(X^2-1)\,Y^4-3(5X^2+1)(X^2+5)\,Y^2+(X^2-1)^3 = 0, \tag{3.13}$$

it can be shown that this equation always has three real roots for Y^2, and that if $X^2 < 1$ only one of these is positive, and that if $X^2 > 1$ two of them are positive. Thus the caustic, which is clearly symmetric about $Y = 0$, has two branches if $X^2 > 1$ and one if $X^2 < 1$. Near the point A_1 in figure 2(*a*) the curve is parabolic with $Y-1 \sim \frac{1}{6}X^2$, and near the point B_1 it has the form of a semi-cubical parabola with $27\,Y^2 \sim 2(|X|-1)^3$. From (3.11) we see that the curve has the lines $8\,Y^2 = X^2$ as

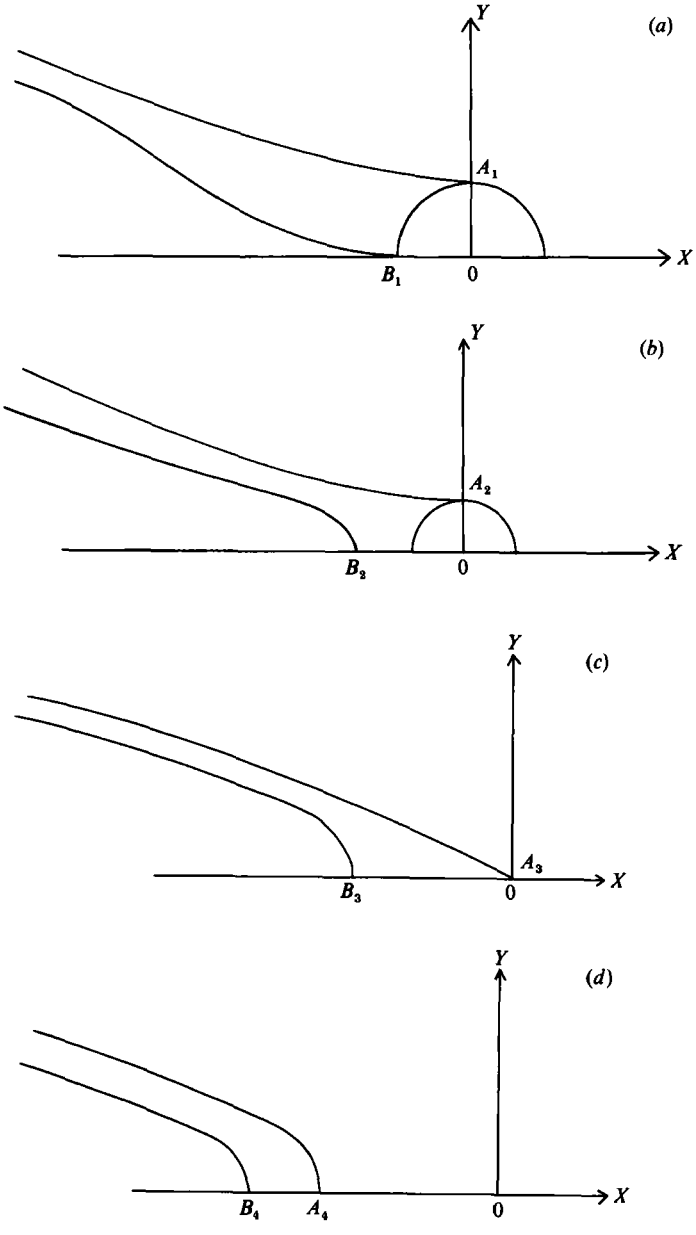

FIGURE 2. Sketch of the far-field caustic for (*a*) $\bar{\theta} = 0$, (*b*) $0 < \bar{\theta} < 1$, (*c*) $\bar{\theta} = 1$ and (*d*) $\bar{\theta} > 1$. In (*a*) the circle has radius unity, and in (*b*) $(1-\bar{\theta})^{\frac{1}{2}}$. Refer to definitions of $\bar{\theta}$, X and $\bar{Y}$ given in (3.1).

asymptotes but never crosses these lines. Indeed neither does it cross the hyperbola $8Y^2 - X^2 = 5$, so that $8Y^2 - X^2 - 5 > 0$ on the upper branch (through the point A_1) and is < 0 on the lower branch (through the point B_1). It therefore follows from (3.12*a*, *b*) that $\lambda_c > 0$ on the lower branch and $\lambda_c < 0$ on the upper branch. Thus the two positive roots of (3.7) coincide on the lower branch but the two negative roots survive as real roots until the upper branch is attained. The curve is sketched for $X \leqslant 0$ and $Y \geqslant 0$ in figure 2(*a*), together with the semicircle $X^2 + Y^2 = 1$, the reason

for which is explained below. Sketched also in figure 2 (*b*, *c*, *d*) are the curves obtained by rotating those in figure 2 (*a*) about the X-axis and cutting the resulting body of revolution with the plane $Z = \overline{\theta}^{\frac{1}{2}}$. In figure 2 (*b*), $\overline{\theta} < 1$ and the semicircle has radius $(1-\overline{\theta})^{\frac{1}{2}}$ and the curves apart from the circle make up the caustic; near the point A_2, $Y^2 \sim 1-\overline{\theta}+\frac{1}{3}X^2$ and the position of the point B_2 is obtained, if required, by solving (3.13) for X with $Y^2 = \overline{\theta}$. For example, if $\overline{\theta} \ll 1$, B_2 is $\{-1-3(2\overline{\theta})^{\frac{1}{3}}, 0\}$. In figure 2 (*c*), $\overline{\theta} = 1$ and the branch of the curve through the origin has slope $3^{-\frac{1}{2}}$ there; the point B_2 is $(-3^{\frac{1}{2}}, -6^{\frac{1}{2}}, 0)$. In figure 2 (*d*), $\overline{\theta} > 1$ and if, for example, $\overline{\theta} \gg 1$, the points A_4, B_4 are $(-2^{\frac{3}{2}}\overline{\theta}^{\frac{1}{2}} \pm 3^{\frac{1}{2}}, 0)$ respectively. In figure 2 (*d*), the point A_4 may be regarded as defining the tilting angle of the caustic. In the limit $\overline{\theta} \to \infty$ the result, $X \sim -2^{\frac{3}{2}}\overline{\theta}^{\frac{1}{2}}$, is exactly that of Redekopp (1975) for the steadily moving obstacle.

3.3. *Presence of inertial waves ahead of the obstacle for* $\overline{\theta} < 1$

We now explain the significance of the semicircles in figure 2 (*a*, *b*) and show that, apart from the region interior to this circle, there are no real roots for $\lambda \equiv \overline{\omega}-1$ with $X > 0$. First, it follows from (3.4) and (3.3) that

$$-X = \frac{\lambda(1+\lambda)+\lambda^2-\overline{Y}^2}{|\lambda^2-\overline{Y}^2|^{\frac{1}{2}}} \operatorname{sgn}[\lambda(1+\lambda)], \tag{3.14}$$

where we have made use of the fact that the real roots of (3.6) have $\lambda^2 > \overline{Y}^2$. It is clear from (3.14) that $X < 0$ when $\lambda > 0$, so that the positive roots inside the lower branch of the caustic are applicable only behind the body. The same statement is true for the negative roots if $\lambda(1+\lambda) > 0$. If, however, $-1 < \lambda < 0$ and also $\lambda(1+\lambda)+\lambda^2-\overline{Y}^2 > 0$, it is possible for $X > 0$. This can be illustrated with relative ease by considering the roots of (3.7) when $\overline{\theta} = 0$ and $|Y| \ll 1$.

A thorough examination on the existence of real roots for λ in various regions of the caustic behind the semicircle $X^2+Y^2 = 1-\overline{\theta}$ is presented in the Appendix. We summarize the results as follows: (3.7) subject to (3.14) has four real values of λ below the lower branch of the caustic when $X < 0$, two (negative) values of λ between the two branches of the caustic if $X^2+\overline{Y}^2 \geqslant 1$ and $X < 0$, and one (negative) value of λ in $X^2+\overline{Y}^2 < 1$ both for X positive and X negative. Thus for sufficiently large p, i.e. $\overline{\theta} < 1$ or $\Omega > N$, some of the 'lee waves' are present upstream of the obstacle.

3.4. *Stationary-phase result*

In the regions away from the caustic curves and the circle $X^2+Y^2 = 1-\overline{\theta}$ the contributions from the saddle points to (2.9) may be written in the usual way. In the variables defined by (3.1), (2.9) becomes

$$\overline{\psi} = \frac{\mathrm{i}p^2}{4\pi^2}\int_{-\infty}^{\infty}\int_{-\infty}^{\infty} F(p\overline{\omega}, p\overline{\sigma})\frac{((\overline{\omega}-1)^2-\overline{\theta})^{\frac{1}{2}}}{(\overline{\omega}^2+\overline{\sigma}^2)^{\frac{1}{2}}} \times \exp\{\mathrm{i}[\overline{\omega}X+\overline{\sigma}Y+((\overline{\omega}-1)^2-\overline{\theta})^{\frac{1}{2}}(\overline{\omega}^2+\overline{\sigma}^2)^{\frac{1}{2}}]p^2\hat{z}\}\,\mathrm{d}\overline{\omega}\,\mathrm{d}\overline{\sigma}. \tag{3.15}$$

To evaluate the contribution from a particular saddle point we need the value of the discriminant which, with Φ as defined in (3.2), is calculated after some algebra to be

$$\left(\frac{\partial^2\Phi}{\partial\overline{\omega}\,\partial\overline{\sigma}}\right)^2 - \frac{\partial^2\Phi}{\partial\overline{\omega}^2}\frac{\partial^2\Phi}{\partial\overline{\sigma}^2} = \frac{[(3\lambda+1)\overline{Y}^2-2\lambda^3]}{(1+\lambda)(\lambda^2-\overline{\theta})} \tag{3.16}$$

at any value of $\lambda(=\overline{\omega}-1)$ and corresponding $\overline{\sigma}$ for which Φ is stationary. It is not difficult to show that the expression in the square brackets vanishes on the caustic curve when $\lambda = \lambda_c$. A typical contribution $\overline{\psi}_s$ from a saddle point to the integral in

(3.15) is of the form, written here for a saddle point $\lambda = \lambda_0$ with $\lambda_0 > 0$, a negative discriminant and a positive value of $\partial^2\Phi/\partial\overline{\sigma}^2$,

$$\overline{\psi}_s = -\frac{F(p\overline{\omega}_0, p\overline{\sigma}_0)(\lambda_0^2-\overline{\theta})^{\frac{1}{2}}(\lambda_0^2-\overline{Y}^2)^{\frac{1}{2}}}{\pi\hat{z}(1+\lambda_0)^{\frac{1}{2}}[2\lambda_0^3-(3\lambda_0+1)\overline{Y}^2]^{\frac{1}{2}}}\exp[ip^2\hat{z}\Phi(\omega_0,\sigma_0)], \tag{3.17}$$

where $\omega_0 = 1+\overline{\lambda}_0$, σ_0 is to be calculated from (3.4*b*), and Φ is defined in (3.2). The sum of such contributions must be taken. Far downstream, where $Y/|X| \ll 1$, the dominant wave is derived from (3.17) as

$$\overline{\psi}_s \approx -\frac{1}{2^{\frac{1}{2}}\pi\hat{z}}F\left(\frac{-x'}{2\hat{z}'}\frac{-y}{\hat{z}}\right)\exp\left(-\frac{i}{4}\frac{x'^2}{\hat{z}}\right), \tag{3.18}$$

which is exactly of the form obtained in I for $p = 0$ and also by Cheng & Johnson (1982) for a homogeneous fluid. It exhibits the same decay as the Fourier transform of the obstacle shape does with ω, σ.

The treatment of the caustic region is standard, see for example I, Cheng (1977) or Cheng & Johnson (1982), and will not be included in detail here. The result is that there is a caustic region of width $O(\hat{z}^{-\frac{2}{3}})$ surrounding both branches of the caustic curve and that the contribution of these regions to the asymptotic expansion of (3.15) is $O(\hat{z}^{-\frac{5}{6}})$. This contribution is described by an Airy function as expected and exhibits exponential decay upstream away from the caustic and oscillatory decay into the region bounded by the caustic curves.

The integral (3.15) has also for large $\hat{z}$, in addition to the oscillatory saddle-point contributions, a non-oscillatory algebraically decaying contribution that is also $O(\hat{z}^{-1})$. In the next section, we calculate this contribution, which is valid both upstream and downstream of the caustic, and show that it is singular on the circle $X^2+\overline{Y}^2 = 1$.

4. The far-field cyclonic disturbance

The origin $\overline{\omega} = \overline{\sigma} = 0$ gives a contribution to the integral (3.15) that is of the same order of magnitude, $O(\hat{z}^{-1})$, as that due to the saddle points to which it must be added in the region downstream of the caustic, and is, by itself, the largest contribution upstream of the caustic. In an initial-value problem this cyclonic pattern asserts itself before the lee-wave pattern is established because, as shown by Hefazi (1985), it is the low wavenumbers that dominate at small values of the time.

When $\overline{\theta} > 1$ this contribution to (3.15) is non-singular, because the origin falls in the evanescent domain and is therefore not a possible position of a saddle (stationary) point (as they occur for $\overline{\omega} > 1+\overline{\theta}$ and $\overline{\omega} < 1-\overline{\theta}$ only). Thus there is no coincidence of saddle point and the phase singularity at the origin. We define

$$V = \int_{-\infty}^{\infty}\int_{-\infty}^{\infty} Z_w(x', y)\,dx'\,dy. \tag{4.1}$$

Then, since the dominant contribution comes from the neighbourhood of the origin, when $\hat{z} \gg 1$,

$$\overline{\psi} \sim \frac{Vp^2}{4\pi^2}\int_{-\infty}^{\infty}\int_{-\infty}^{\infty}\frac{(\overline{\theta}-1)^{\frac{1}{2}}}{(\overline{\omega}^2+\overline{\sigma}^2)^{\frac{1}{2}}}\exp\{[i\overline{\omega}X+i\overline{\sigma}Y-(\overline{\theta}-1)^{\frac{1}{2}}(\overline{\omega}^2+\overline{\sigma}^2)^{\frac{1}{2}}]p^2\hat{z}\}\,d\overline{\omega}\,d\overline{\sigma}, \tag{4.2}$$

which, after a change to polar coordinates in the $(\bar{\omega}, \bar{\sigma})$-plane, may therefore be evaluated as an end-point contribution, yielding

$$\bar{\psi} \sim -\frac{V}{2\pi\hat{z}[1+(X^2+Y^2)/(\bar{\theta}-1)]^{\frac{1}{2}}}, \quad \hat{z} \gg 1. \tag{4.3}$$

Thus as was the case in I with $p = 0$ we have an algebraically decaying cyclonic disturbance that is symmetric about the $\hat{z}$-axis and, unlike the lee waves contributed by the saddle points, has no bias in the downstream direction.

When $\bar{\theta} < 1$, instead of (4.2) we have

$$\bar{\psi} \sim \frac{-\mathrm{i}Vp^2}{4\pi^2} \int_{-\infty}^{\infty} \int_{-\infty}^{\infty} \frac{(1-\bar{\theta})^{\frac{1}{2}}}{(\bar{\omega}^2+\bar{\sigma}^2)^{\frac{1}{2}}} \exp\{\mathrm{i}[\bar{\omega}X+\bar{\sigma}Y-(1-\bar{\theta})^{\frac{1}{2}}(\bar{\omega}^2+\bar{\sigma}^2)^{\frac{1}{2}}]p^2\hat{z}\}\,\mathrm{d}\bar{\omega}\,\mathrm{d}\bar{\sigma}, \tag{4.4}$$

which although falling in the propagating-wave range cannot be treated by the saddle-point method. Again, it can easily be evaluated as an end-point contribution after changing to the polar coordinates as, when $\hat{z} \gg 1$,

$$\bar{\psi} \sim -\frac{\mathrm{i}V}{2\pi\hat{z}[(X^2+Y^2)/(1-\bar{\theta})-1)]^{\frac{1}{2}}}, \quad X^2+Y^2 > 1-\bar{\theta}, \tag{4.5a}$$

$$\bar{\psi} \sim -\frac{V}{2\pi\hat{z}[1-(X^2+Y^2)/(1-\bar{\theta})]^{\frac{1}{2}}}, \quad X^2+Y^2 < 1-\bar{\theta}. \tag{4.5b}$$

Thus the magnitudes of pressure and velocity perturbations amplify as the circle $X^2+Y^2 = 1-\bar{\theta}$ is approached, while the (instantaneous) streamlines would make sharp turns in crossing the circle owing to the phase jump shown in (4.5). When $\bar{\theta} = 1$ it may be shown that the contribution analogous to (4.5) is $O(\hat{z}^{-\frac{3}{2}})$ instead of $O(\hat{z}^{-1})$.

When $\bar{\theta} < 1$ (i.e. $\Omega > N$) the singularity in the neighbourhood of the circle $X^2+Y^2 = 1-\bar{\theta}$ leads to a disturbance of larger magnitude $O(\hat{z}^{-\frac{3}{4}})$, rather than $O(\hat{z}^{-1})$. This neighbourhood is identified by

$$X^2+Y^2 = (1-\bar{\theta})[1+O(p^{-1}\hat{z}^{-\frac{1}{2}})].$$

As this disturbance represents the largest magnitude in the far field, we examine its analytic form in the following section.

5. The dominant contribution to the far fields in the supercritical case

When $0 \leqslant \bar{\theta} \leqslant 1$, the largest contribution, $O(\hat{z}^{-\frac{3}{4}})$, to the far-field disturbance is, as we shall now demonstrate, concentrated in the neighbourhood of the circle $X^2+Y^2 = 1-\bar{\theta}$ and is associated with both types of asymptotic behaviour so far discussed, the 'lee waves' of §3 and the cyclonic disturbance of §4. It is evident from (4.5) that the cyclonic disturbance becomes singular on the boundary of the circle and we recall from §3 that one of the saddle points of (3.15) responsible for the lee waves is transferred from a position behind the body to one in front of it, as this circle is entered from the outside. This is the saddle point associated with the root λ_1, of (3.7). In the region where

$$Q \equiv p\hat{z}^{\frac{1}{2}}\left(\frac{X^2+Y^2}{1-\bar{\theta}}-1\right) = O(1), \tag{5.1}$$

both effects are of the same size and the resulting disturbance in this neighbourhood arises from a coincidence of the saddle point with $\lambda_1 = -1$ and of the origin in the $(\bar{\omega}, \bar{\sigma})$-plane.

We first discuss the form that $\bar{\psi}$ must take as $|Q| \to \infty$ in order that the solution where $|Q| = O(1)$ may match with the solutions already obtained inside and outside the circle. Apart from the neighbourhoods of the caustic curves, where it rises to $O(\hat{z}^{-\frac{5}{6}})$, the disturbance is $O(\hat{z}^{-1})$ and is obtained by adding the contribution from (4.5) to that from the saddle points as exemplified by (3.17). The expression for $\bar{\psi}$ that we obtain when $Q = O(1)$ must have the following properties. If $X < 0$, then as $Q \to \infty$, $\bar{\psi}$ must contain two oscillatory lee-wave components (corresponding to both roots λ_1, λ_2) and an algebraic cyclonic component; when $Q \to -\infty$, $\bar{\psi}$ must contain one oscillatory component (that corresponding to the root λ_2 only) in addition to the algebraic component. If $X > 0$, then as $Q \to \infty$, $\bar{\psi}$ must contain an algebraic component only, though as $Q \to -\infty$ it must also contain the appropriate oscillatory component derived from the root λ_1.

These matching requirements are obtained by letting $\lambda \to -1$ in the expression (3.16) for the discriminant and calculating the limiting form of the saddle-point contribution as $X^2 + Y^2 \to 1 - \bar{\theta}$. With the addition of the algebraic contributions calculated from (4.5) we obtain the requirements that if $X < 0$ then

$$\bar{\psi} \sim -\frac{Vp^{\frac{1}{2}}}{\pi \hat{z}^{\frac{3}{4}} Q^{\frac{1}{2}}} \exp\left[\frac{-\mathrm{i}(1-\bar{\theta})^2 Q}{16X}\right] - \frac{\mathrm{i}Vp^{\frac{1}{2}}}{2\pi \hat{z}^{\frac{3}{4}} Q^{\frac{1}{2}}} + \bar{\psi}_1, \quad \text{as } Q \to \infty, \tag{5.2a}$$

$$\bar{\psi} \sim -\frac{Vp^{\frac{1}{2}}}{2\pi \hat{z}^{\frac{3}{4}} |Q|^{\frac{1}{2}}} + \bar{\psi}_1, \quad \text{as } Q \to -\infty, \tag{5.2b}$$

where $\bar{\psi}_1$ is the oscillatory contribution from the root λ_2, which remains $O(\hat{z}^{-1})$ throughout the circle for $X < 0$ and does not occur if $X > 0$. If $X > 0$

$$\bar{\psi} \sim -\frac{\mathrm{i}Vp^{\frac{1}{2}}}{2\pi \hat{z}^{\frac{3}{4}} Q^{\frac{1}{2}}} + \bar{\psi}_1, \quad \text{as } Q \to \infty, \tag{5.3a}$$

$$\bar{\psi} \sim -\frac{\mathrm{i}Vp^{\frac{1}{2}}}{\pi \hat{z}^{\frac{3}{4}} |Q|^{\frac{1}{2}}} \exp\left[\frac{-\mathrm{i}(1-\bar{\theta})^2 Q}{16X}\right] - \frac{Vp^{\frac{1}{2}}}{2\pi \hat{z}^{\frac{3}{4}} Q^{\frac{1}{2}}}, \quad \text{as } Q \to -\infty. \tag{5.3b}$$

To obtain the form of $\bar{\psi}$ when $Q = O(1)$ and $\hat{z} \gg 1$ that has the properties (5.2) and (5.3) we find that it is sufficient to consider (3.15) as

$$\bar{\psi} \sim -\frac{\mathrm{i}Vp^2(1-\bar{\theta})^{\frac{1}{2}}}{4\pi^2} \int_0^{2\pi} \int_0^{\infty} \exp\{\mathrm{i}r[X\cos\phi + Y\sin\phi - |(r\cos\phi - 1)^2 - \bar{\theta}|^{\frac{1}{2}}] p^2 \hat{z}\} \, \mathrm{d}r \, \mathrm{d}\phi, \tag{5.4}$$

on setting $\bar{\omega} = r\cos\phi$, $\bar{\sigma} = r\sin\phi$ and giving the multiplier in front of the exponential its value at $\bar{\omega} = 0$. We are interested in small values of r with $Q = O(1)$ and we denote the exponent in the integrand in (5.4) by $\mathrm{i}p^2 \hat{z} K(r, \phi)$. Now

$$K(r, \phi) = r\left\{X\cos\phi + Y\sin\phi - (1-\bar{\theta})^{\frac{1}{2}} + \frac{r\cos\phi}{(1-\bar{\theta})^{\frac{1}{2}}}\right\} + O(r^3) \tag{5.5}$$

and upon setting

$$\left.\begin{aligned} r(1-\bar{\theta})^{\frac{1}{2}} = r_1, \quad X = X_1(1-\bar{\theta})^{\frac{1}{2}}, \quad Y = Y_1(1-\bar{\theta})^{\frac{1}{2}}, \\ R_1^2 = \left(X_1 + \frac{r_1}{(1-\bar{\theta})^{\frac{1}{2}}}\right)^2 + Y_1^2, \end{aligned}\right\} \tag{5.6}$$

we consider, from (5.4),

$$\overline{\psi} \sim -\frac{\mathrm{i}Vp^2(1-\overline{\theta})^{\frac{1}{2}}}{2\pi^2}\int_0^{\pi}\int_0^{\infty} \exp\left[\mathrm{i}r_1(R_1\cos\phi_1 - 1)p^2\hat{z}\right]\mathrm{d}r_1\,\mathrm{d}\phi_1, \tag{5.7}$$

where ϕ_1 is related to ϕ by an origin shift and the terms $O(r^3)$ in $K(r,\phi)$ have been ignored. When $X_1^2+Y_1^2=1$ the integrand in (5.7) has its saddle point at $r_1=0, \phi_1=0$ and when $X_1^2+Y_1^2 = 1+Qp^{-1}\hat{z}^{-\frac{1}{2}}$ the saddle point is at $\phi_1 = O(z^{-1})$, $r_1 = -(1-\overline{\theta})^{\frac{3}{2}}Q/(4pX_1\hat{z}^{\frac{1}{2}})$, which is in agreement with our earlier findings that the saddle point whose position tends to $X_1^2+Y_1^2=1$ as $\lambda_1\to -1$ exists outside the circle if $X_1<0$, and inside if $X_1>0$. In (5.7) we expand the integrand for small r_1, ϕ_1, retain the dominant terms and write

$$r_1 = \frac{1}{p\hat{z}^{\frac{1}{2}}} - \frac{1}{4}\frac{(1-\overline{\theta})^{\frac{3}{2}}}{X_1}Q + s_1, \quad \phi_1 = \frac{1}{p^{\frac{1}{2}}\hat{z}^{\frac{1}{4}}}\tilde{\phi}. \tag{5.8}$$

This leads to

$$\overline{\psi} \sim -\frac{\mathrm{i}Vp^{\frac{1}{2}}}{2\pi^2\hat{z}^{\frac{3}{4}}}\int_{\nu Q}^{\infty}\int_0^{\infty} \exp\left\{\mathrm{i}\left[-\frac{\nu}{4}Q^2 - \tfrac{1}{2}(s_1-\nu Q)\tilde{\phi}^2 + s_1^2 X_1(1-\overline{\theta})^{-\frac{3}{2}}\right]\right\}\mathrm{d}\tilde{\phi}\,\mathrm{d}s_1, \tag{5.9}$$

where $\nu = (1-\overline{\theta})^{\frac{3}{2}}/(4X_1)$, and (5.9) may be reduced to the single integral

$$\overline{\psi} \sim -\frac{V\,\mathrm{e}^{\mathrm{i}\pi/4}p^{\frac{1}{2}}}{(2\pi)^{\frac{3}{2}}\hat{z}^{\frac{3}{4}}}\,\mathrm{e}^{-\mathrm{i}\nu Q^2/4}\int_{\nu Q}^{\infty}\frac{\exp\left[\mathrm{i}s_1^2 X_1(1-\overline{\theta})^{-\frac{3}{2}}\right]}{(s_1-\nu Q)^{\frac{1}{2}}}\mathrm{d}s_1. \tag{5.10}$$

This gives the asymptotic form of (3.15) for large $\hat{z}$ in the region where $Q = O(1)$.

That (5.10) takes the required forms (5.2) and (5.3) as $|Q|\to\infty$ for $X<0$ and $X>0$ respectively may be shown by finding its asymptotic expansions as $Q\to\pm\infty$. If $|Q|\gg 1$ and $QX_1<0$ the saddle point at the origin lies in the range of integration and gives a contribution in addition to that from the end point $s=\nu Q$. Together these give (apart from ϕ_1 which is $O(\hat{z}^{-1})$) exactly (5.2*a*) and (5.3*b*). However if $|Q|\gg 1$ and $QX_1>0$ the saddle point lies outside the range of integration and we obtain (5.2*b*) and (5.3*a*). Thus the maximum strength of $\overline{\psi}$ around the circle is theoretically established as $O(\hat{z}^{-\frac{3}{4}})$, which is of an order lower than that in the caustic transition zone, $O(\hat{z}^{-\frac{5}{6}})$.

In fact the largest contribution to $\overline{\psi}$ in (3.15) comes from the neighbourhood of the points A_1, A_2 in figures 2(*a*, *b*). Since these points are at the junction of the circle and the caustic, this is not surprising. Near A_1, A_2 where $\overline{Y}^2\sim 1$ and $|X|\ll 1$ it is necessary to retain the terms $O(r^3)$ in (5.5). In the case $\overline{\theta}=0$ for example, we have, from (5.7), to replace (5.9),

$$\begin{aligned}\overline{\psi} &\sim -\frac{\mathrm{i}Vp^2}{2\pi^2}\int_0^{\infty}\int_0^{\infty}\exp\left[\frac{\mathrm{i}r}{2}(Y^2-1+2Xr+r^2-\phi_1^2)p^2\hat{z}\right]\mathrm{d}r\,\mathrm{d}\phi_1\\ &= -\frac{Vp\,\mathrm{e}^{\mathrm{i}\pi/4}}{(2\pi)^{\frac{3}{2}}\hat{z}^{\frac{1}{2}}}\int_0^{\infty}\exp\left[\frac{\mathrm{i}r}{2}(Y^2-1+2Xr+r^2)p^2\hat{z}\right]\frac{\mathrm{d}r}{r^{\frac{1}{2}}},\end{aligned} \tag{5.11}$$

which gives a contribution $O(\hat{z}^{-\frac{3}{4}})$ in a region where $Y^2-1 = O(\hat{z}^{-\frac{2}{3}})$, $|X| = O(\hat{z}^{-\frac{1}{3}})$.

6. Examples

It is the appearance of a circle of maximum amplitude, along with a phase jump, that may be considered as the outstanding feature distinguishing the far field of the supercritical case. To illustrate their occurrence for a particular topography, the

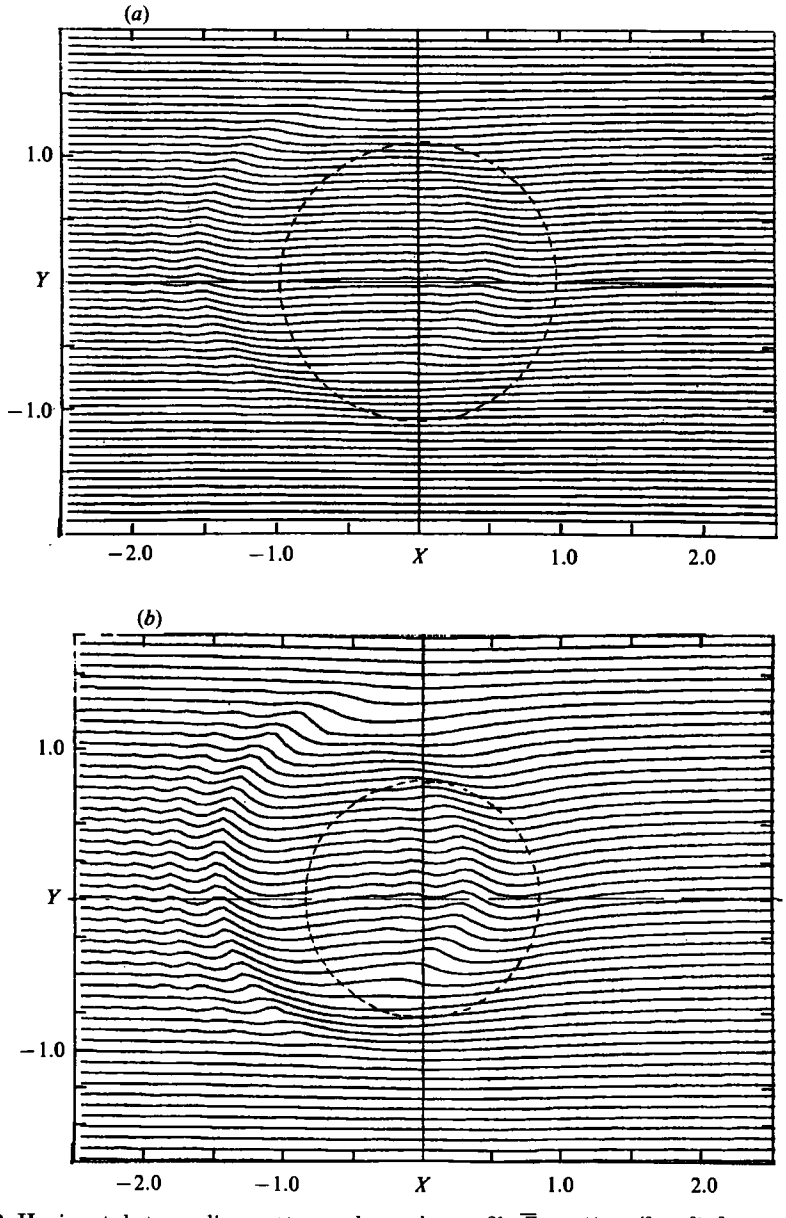

FIGURE 3. Horizontal streamline patterns above the profile $\overline{Z}_w = (1+x'^2+y^2)^{-2}$ at a reduced height $\hat{z} = 2.0$ and a reduced frequency $p = 5.0$ for (*a*) $\overline{\theta} = 0$ and (*b*) $\overline{\theta} = 0.2$. The value of τ is 0.25 in each case and that of pt is 2π. In (*a*) the circle has radius unity, and in (*b*) $2/5^{\frac{1}{4}}$.

instantaneous streamlines have been calculated from (4.2) for flow past the profile

$$\overline{Z}_w(x', y) = (1+x'^2+y^2)^{-2}, \tag{6.1}$$

when it is regarded as stationary with respect to the (x', y)-coordinates. The method of computation was that of a fast-Fourier-transform algorithm as used in I. For illustration, two values of $\overline{\theta}$ corresponding to the supercritical cases were taken, namely $\overline{\theta} = 0$ and $\overline{\theta} = 0.2$, both with $p = 5$ and $\hat{z} = 2$. The results for a value $\tau = 0.25$ of the non-dimensional thickness ratio are presented in figure 3 (*a*, *b*) for the instant

when pt is a multiple of 2π. In I, the same profile (6.1) was considered with $p = 0$ and $\hat{z} = 0.5$, in which case the cyclonic disturbance was clearly visible in the streamline pattern. Here $\hat{z}$ is fourfold greater and the only remaining visible perturbation is the largest that occurs, namely that in the neighbourhood of the boundary of the circle $X^2 + Y^2 = 1 - \bar{\theta}$, which is $O(\hat{z}^{-\frac{3}{4}})$ according to §5. In both figures the appropriate circle is shown by a dotted line (not quite circular as the X- and Y-scales differ slightly). As predicted, the oscillatory disturbance is concentrated on the inside of the boundary for $X > 0$ (i.e. ahead of the body) and on the outside for $X < 0$. However, at this value of $\hat{z}$, the pattern is still somewhat downstream of its final asymptotic position though, in particular in figure 3(*b*), it is possible to detect the increase in amplitude, to $O(\hat{z}^{-\frac{3}{8}})$, in the neighbourhood of the points whose asymptotic positions will be $X = 0$, $Y = \pm(1-\bar{\theta})^{\frac{1}{2}}$ corresponding to A_2 in figure 2(*b*). The 'lee waves' bounded by the outer caustic of §3 but downstream of the circle are too weak in this case to be detected at this height.

7. Discussion

We have analysed the effect of surface undulation on the flow field about an obstacle in uniform motion at the base of a deep, rapidly rotating container, in which the fluid is linearly stratified. The problem, linearized for a thin obstacle corresponding to a shallow topography, has been solved for a single sinusoidal temporal mode e^{ipt} for an arbitrary p, furnishing therefore the frequency response to a Fourier component in the frequency spectrum of a more general unsteady motion, as permitted by the requirements $\tau \ll 1$ and $p = O(1)$. In this sense, the restriction to a sinusoidal oscillation may find its relevance. The results and extension of this study have merit in their own right, as will be discussed further below.

7.1. *Frequency threshold*

The result of I for the steady case ($p = 0$) has shown that, except in the homogeneous limit ($\theta = 0$), a large-scale, solitary, and symmetrically distributed cyclonic disturbance is generally present in the far field and hence coexists with the ship-wave like pattern of the more familiar inertial lee waves. For unsteady motions ($p \neq 0$), the analysis of §§3 and 4 shows that the solitary cyclonic feature is present for *all* degrees of stratification with no exception (including the homogeneous limit $\theta = 0$), but the far-field pattern is found to depend critically on the relative magnitude of the pulsating and Brunt–Väisälä frequencies, i.e. on $\bar{\theta} \equiv \theta/p^2 = (N/\Omega)^2$. More significant perhaps are the existence of a threshold frequency at $\Omega = N$ which is independent of the background rotation, and the 'circle of maximum disturbance' with accompanying features in both the cyclonic and the wave patterns at a supercritical frequency ($\Omega > N$). Whereas a frequency threshold also exists in the classical theory of internal gravity waves (Yih 1980, pp. 60–67), its occurrence at the same N under a strong Coriolis influence may seem rather surprising.

7.2. *Lee waves and caustics*

Unlike the steady case, two (inner and outer) branches of far-field caustics are found, within and downstream of which the familiar inertial waves are confined. Two more branches, forming the two halves of a full circle (a conical surface with circular cross-section, to be more precise) must however be added in the supercritical case. In spite of this complication, the variety of caustic geometries is recognized to be

related simply to those in the homogeneous limit. While it is apparent that the circular caustic forms an upstream barrier for propagating wavetrains ahead (and above) of the obstacle, the presence of the upstream 'lee waves' can be confirmed only if their existence is established from the solution; this has been accomplished at the end of §3.

7.3. *Cyclonic disturbance as large-scale feature*

As noted, the stationary-phase method applied in §3 precludes the contribution of the singularities of the phase, particularly that at the wavenumber origin $\omega = \sigma = 0$. Its contribution to the pressure is determined in §4 to yield a large-scale cyclonic pattern of disturbance, with a magnitude generally of the order $\hat{z}^{-1}$, the same as that describing the inertial lee-wave system, when $\overline{\theta} = O(1)$. This cyclonic feature could have been anticipated by consideration of the solution to the governing equations (2.6) and (2.7) for horizontal scales *much* longer than that required by the inertial lee waves. In this case, the convective derivative $\partial/\partial x'$ in $(\partial/\partial t - \partial/\partial x')^2$ becomes unimportant and the second term in the inner boundary conditions (2.7) can be replaced by a double delta function in the (x', y)-plane. Specializing to a Fourier temporal mode, (2.6) and (2.7) may then be simplified to

$$\left[\frac{\partial^2}{\partial \hat{z}^2} + (\theta - p^2)\left(\frac{\partial^2}{\partial x'^2} + \frac{\partial^2}{\partial y^2}\right)\right]\overline{\psi} = 0, \tag{7.1a}$$

$$\frac{\partial \overline{\psi}}{\partial \hat{z}} = -p^2 V \delta(x')\,\delta(y) \quad \text{at } \hat{z} = 0, \tag{7.1b}$$

which, for an algebraically decaying $\overline{\psi}$ at large distances, yield (4.3) and (4.5*a*, *b*). Note that both real and imaginary values of $\overline{\psi}$ must be included in evaluating the real part of $\psi = \overline{\psi}\, e^{ipt}$. On the other hand, to produce the ship-wave-like inertial wave pattern of §4, the relative scales among the time and horizontal scales must remain the same as for the lower altitude, and hence the contribution from $\partial/\partial x'$ in $(\partial/\partial t - \partial/\partial x')^2$ of (2.6) and (2.7) cannot be omitted; this gives a bias in the downstream direction, leading to the closely packed lee-wave pattern. The same consideration can also be used to explain the reduction to the Laplace equation in the work of Hogg (1973, 1980), Ingersoll (1969) and others mentioned earlier, for which p in (7.1) is zero.

7.4. *Prominent far-field features: subcritical case*

At a subcritical frequency ($\Omega < N$), the most dominant feature in the far field is the cyclonic mode (4.3) which is made prominent by the *peak* of its extensive solitary distribution at $X = Y = 0$, even though its magnitude in $|\psi|$ ranks the same as that of the lee waves, namely $O(\hat{z}^{-1})$, and theoretically ranks second to the accumulated strength in the caustic-transition zone $O(\hat{z}^{-\frac{5}{6}})$. The dominance of the cyclonic component is greatly enhanced by a relatively high θ (see (4.3)) while the lee waves and its accumulated strength over the caustic boundary are greatly diminished by an increased θ, owing to the dependence on $F(\omega, \sigma)$ and the increases of the stationary values of ω and σ with θ as $\theta^{\frac{1}{2}}$, as explained in I for the non-oscillatory case $p = 0$. Even for θ as low as unity, the maximum strength of $\overline{\psi}$ at height $\hat{z} = 5$ is still found at the peak $X = Y = 0$ of the cyclonic component when $p = 0$ (cf. figure 4 in I).

7.5. *Prominent far-field features: supercritical case*

In the supercritical case ($\Omega > N$), the largest magnitude of $|\psi|$ in the far field occurs unquestionably in the vicinity of the circle $X^2 + Y^2 = (1 - \overline{\theta})$, and is established to

be $O(\hat{z}^{-\frac{1}{4}})$ in (5.9) in §5; its prominence should be considered a field property of the cyclonic disturbance although it also serves as a barrier to the 'upstream lee waves'. The strength of this ring of maximum disturbance reaches the peak at the juncture where the outer caustic joins the circle (cf. figures 2*a*, *b*) and the magnitude of $\overline{\psi}$ is shown to further increase to $O(\hat{z}^{-\frac{1}{3}})$ in (5.11). The examination of the examples from two numerical solutions to the full solution at finite heights made in §6 leaves little doubt of the presence of the features brought out by the asymptotic analysis.

7.6. *Relation to Görtler's studies*

As noted in §1, Görtler (1944, 1957) found a frequency threshold in his studies of a periodic disturbance in a *homogeneous* rotating fluid, for which a linearized equation very similar to (7.1*a*) is applicable, except that, formally, $(\theta - p^2)$ is replaced by $[1 - 4(\Omega_c/\Omega)^2]$. Thus the equation therein is hyperbolic in its spatial dependence for $\Omega < 2\Omega_c$, with the emergence of the characteristic surface

$$x'^2 + y^2 = \hat{z}^2 \Big/ \left[4\left(\frac{\Omega_c}{\Omega}\right)^2 - 1\right], \tag{7.2}$$

as noted in Greenspan (1968). Although $\Omega = 2\Omega_c$ is far beyond the range of Ω considered here for $p = \Omega/\Omega_c \mathscr{R} = O(1)$, one surmises that N and $2\Omega_c$ could remain as the two threshold frequencies even in a *non-geostrophic* domain ($\mathscr{R} \neq 0$). This expectation is encouraged by the agreement of (7.2) with the characteristic surface of the solution (4.5*a*, *b*), for $\overline{\theta} \to 0$ under $\Omega/\Omega_c = p\mathscr{R} \ll 1$.

7.7 *Departure from geostrophy*

In order to answer adequately the question on frequency thresholds for a non-vanishing $\mathscr{R}$, a relaxation from geostrophy in the formulation is necessary. A linearized analysis for this obstacle may then be made for finite $\mathscr{R}$, $\overline{\theta} = (N/\Omega)^2$, and Ω/Ω_c, and will shed light on this question.

The extension to a non-vanishing $\mathscr{R}$ is an interesting one in as much as it may be shown that the frequency cut-off for the propagating wavetrains will occur not only at $\omega = p \pm \theta^{\frac{1}{2}}$ as in (2.12*a*) but also at $\omega = p \pm 2\mathscr{R}^{-1}$ (e.g. Hefazi 1985). The condition

$$\mathscr{R} = 2\theta^{-\frac{1}{2}}, \quad \text{i.e. } N = 2\Omega_c \tag{7.3}$$

is then seen to be more critical than the frequency threshold. For $\mathscr{R} < 2\theta^{-\frac{1}{2}}$, wavetrains with upward-propagating components cover two ranges of ω in (2.11); as $\mathscr{R} \to 2\theta^{-\frac{1}{2}}$, the windows for these two wavetrains vanish, leaving the large-scale, cyclonic disturbance to be the only major feature in the far field (for all p); when $\mathscr{R}$ exceeds $2\theta^{-\frac{1}{2}}$, windows for the upward-propagating waves reopen. From this and a consideration of (2.6) generalized to $\mathscr{R} \neq 0$ for the large-scale disturbance, one may readily infer the condition for the appearance of the circle of maximum disturbance to be

$$\begin{aligned} \theta^{\frac{1}{2}} < p < 2/\mathscr{R}, &\quad \text{if } \mathscr{R} < 2\theta^{-\frac{1}{2}}, \\ 2/\mathscr{R} < p < \theta^{\frac{1}{2}}, &\quad \text{if } \mathscr{R} > 2\theta^{-\frac{1}{2}}, \end{aligned}$$

which are equivalent to

$$\left.\begin{aligned} N < \Omega < 2\Omega_c &\quad \text{if } N < 2\Omega_c, \\ 2\Omega_c < \Omega < N &\quad \text{if } 2\Omega_c < N. \end{aligned}\right\} \tag{7.4}$$

Thus N and $2\Omega_c$ are indeed the frequency thresholds for the supercritical flow structure, for *all* $\mathscr{R}$, *irrespective* of whether $N \gtrless 2\Omega_c$.

The foregoing discussion on the frequency thresholds does not however indicate a complete independence of the solution of the Rossby number, which controls the convective inertial influence. To determine correctly some of the important flow details, as well as establishing more firmly the foregoing conclusion, a thorough analysis with $\mathscr{R} \neq 0$ parallel to §§3, 4, 5 should yield results of both theoretical and practical interest. In particular, the drag and side force affecting the overall momentum and energy balances in the present problem will be decisively controlled by the $\theta^{\frac{1}{2}}$ and $\mathscr{R}$ which, together with p, determine the window for the outward-propagating waves, and hence the rate of radiation loss. As noted earlier, the outgoing waves disappear when $\theta^{\frac{1}{2}}\mathscr{R} = N/\Omega_c = 2$ and the drag vanishes, as has been substantiated by an analysis for $\mathscr{R} \neq 0$ in the steady case (Hefazi 1985). How a periodic cyclonic motion may affect the far-field energy balance at $\mathscr{R} = 2\theta^{-\frac{1}{2}}$ and other $\mathscr{R}$ is not altogether clear.

The presence of the circle of maximum disturbance implies a directional preference in the propagation of the inertial-baroclinic waves at a supercritical frequency. The results established in §§4 and 5 could help in estimating the geophysical influence on oceanic data gathered through remote sensing. To be useful, however, it is again essential to extend the analysis to a non-vanishing $\mathscr{R}$, in as much as the length and time scales required by $\mathscr{R} \ll 1$ for geostrophy may be too large to be meaningful in an atmospheric application.

Apart from its limitation due to a small $\mathscr{R}$, the present theory has also omitted the important Ekman pumping and a variety of viscous phenomena in rotating flows (see Greenspan 1968). Of great consequence is the possibility of wake generation from the Taylor column above and close to an obstacle, such as a (shallow) truncated cylinder or a (thin) spherical cap. The experimental and theoretical evidence of its occurrence have been brought out in Boyer (1970) and Walker & Stewartson (1974), and are also discussed in Stewartson & Cheng (1979).

The authors are grateful to Dr H. Hefazi for his help in the numerical inversion from which figure 3(*a*, *b*) was derived. This research was supported by the United States National Science Foundation Engineering Division, Fluid Mechanics Program under grant number NSF MEA-82-17-835.

Appendix. Upstream 'lee waves' for $0 \leqslant \bar{\theta} < 1$

We now show the existence of 'lee waves' for $0 \leqslant \bar{\theta} < 1$ inside the circle $X^2 + Y^2 = 1 - \bar{\theta}$ both for positive and negative X. Let λ_1, λ_2 be the two negative roots of (3.7) and first note, from (3.6), since $\lambda^2 \geqslant \bar{Y}^2$, that if $\bar{Y}^2 > 1$, but is inside the outer branch of the caustic so that λ_1, λ_2 are still real, then λ_1, $\lambda_2 < -1$ and X in (3.13) is negative. It may be argued from (3.7) that one root, λ_1 say, takes the value -1 on $X^2 + \bar{Y}^2 = 1$, inside the circle both λ_1, $\lambda_2 > -1$, and outside the circle except for $\bar{Y}^2 < 1$, we have $\lambda_1 < -1$ and $\lambda_2 > -1$, with $\lambda_2 = -1$ on $\bar{Y} = 1$. For $\bar{Y}^2 \leqslant 1$, the roots are equal only at $X = 0$, $\bar{Y} = 1$, and otherwise $\lambda_1 < \lambda_2$.

When $\bar{Y}^2 = 1$, since $\lambda_1 < -1$, it is clear that the corresponding X in (3.14) is negative, and by setting $\bar{Y}^2 = 1 - \mu$, $|\mu| \ll 1$, we find that $\lambda_2 = -1 + \frac{1}{2}\mu$ so that the corresponding X is also negative in the limit $\bar{Y}^2 \to 1$. If however $\bar{Y}^2 < 1$ whether the X values corresponding to λ_1 and/or λ_2 are positive or negative depends on whether $X^2 + \bar{Y}^2 \gtrless 1$ as we now show.

To demonstrate this we denote the left-hand side of (3.7) by $E(\lambda)$ and assume that $\overline{Y}^2 < 1$ and $X^2 > 0$. Then $E(0) > 0$, $E(-\infty) > 0$ and $E(-1) = (1-\overline{Y}^2)(1-\overline{Y}^2-X^2)$. Also if

$$\Lambda = -\tfrac{1}{4}-\tfrac{1}{2}\overline{Y}^2+\tfrac{1}{16}^{\frac{1}{2}}, \quad \Lambda > -1, \tag{A 1}$$

so that Λ is the root of the quadratic in the numerator of (3.14) which has $\Lambda^2 > \overline{Y}^2$ for $\overline{Y}^2 < 1$, then $E(\Lambda) = X^2(\overline{Y}^2-\Lambda^2) < 0$. Suppose first that $X^2+\overline{Y}^2 > 1$. Then, since $E(-1) < 0$ and $E(\Lambda) < 0$, it follows that $0 > \lambda_2 > \Lambda > -1$ and $\lambda_1 < -1$. Thus for λ_1, X is immediately negative, and the result is also true for λ_2 upon noting that $2\lambda_2^2+\lambda_2-\overline{Y}^2 < 0$, since $\lambda_2 > \Lambda$.

Now suppose that $X^2+\overline{Y}^2 < 1$. Then $E(-1) > 0$, $E(-\infty) > 0$ thus $0 > \lambda_2 > \Lambda > \lambda_1 > -1$, and in (3.14) X is negative for λ_2 but positive for λ_1. Thus the root λ_1 leads to inertial waves in front of the obstacle inside the region $X^2+\overline{Y}^2 = 1$, which would otherwise trail behind $X = 0$ as the familiar lee waves.

REFERENCES

Batchelor, G. K. 1967 *An Introduction to Fluid Dynamics*. Cambridge University Press.

Boyer, D. L. 1970 *J. Fluid Mech.* **50**, 675.

Buzzi, A. & Tibaldi, S. 1977 *Q. J. R. Met. Soc.* **103**, 135.

Cheng, H. K. 1977 *Z. angew. Math. Phys.* **28**, 753.

Cheng, H. K., Hefazi, H. & Brown, S. N. 1984 *J. Fluid Mech.* **141**, 431.

Cheng, H. K. & Johnson, E. R. 1982 *Proc. R. Soc. Lond.* A **383**, 171.

Görtler, H. 1944 *Z. angew. Math. Mech.* **24**, 210.

Görtler, H. 1957 *Proc. 5th Midwestern Conf. Fluid Mech.* 1–10, pp. 3, 10, 192, 202.

Greenspan, H. P. 1968 *The Theory of Rotating Fluids*. Cambridge University Press.

Hefazi, H. 1985 Topographically generated flows and wave patterns in a rotating, stratified fluid. Ph.D. Thesis. University of Southern California.

Heikes, K. E. & Maxworthy, T. 1982 *J. Fluid Mech.* **125**, 319.

Hide, R., Ibbetson, A. & Lighthill, M. J. 1968 *J. Fluid Mech.* **32**, 251.

Hogg, N. G. 1973 *J. Fluid Mech.* **58**, 517.

Hogg, N. G. 1980 Effects of bottom topography on ocean currents. In *Orographic Effects in Planetary Flows*. GARP Publ. Series, vol. 23, p. 169.

Huppert, H. E. 1975 *J. Fluid Mech.* **67**, 397.

Ingersoll, A. P. 1969 *J. Atmos. Sci.* **26**, 744.

Johnson, E. R. 1978 *J. Fluid Mech.* **86**, 209.

Johnson, E. R. 1982 *J. Fluid Mech.* **120**, 359.

Lighthill, M. J. 1965 *J. Inst. Maths Applics* **1**, 1.

Lighthill, M. J. 1967 *J. Fluid Mech.* **27**, 725.

Lighthill, M. J. 1978 *Waves in Fluids*. Cambridge University Press.

Mason, P. J. & Sykes, R. I. 1979 *J. Fluid Mech.* **91**, 433.

Maxworthy, T. 1977 *Z. angew. Math. Phys.* **28**, 853.

Pedlosky, J. 1979 *Geophysical Fluid Dynamics*. Springer.

Redekopp, L. G. 1975 *Geophys. Fluid Dyn.* **6**, 289.

Smith, R. 1979*a* *J. Atmos. Sci.* **36**, 2395.

Smith, R. 1979*b* *Adv. Geophys.* **21**, 87.

Stewartson, K. & Cheng, H. K. 1979 *J. Fluid Mech.* **91**, 415.

Walker, J. D. A. & Stewartson, K. 1974 *J. Fluid Mech.* **66**, 767.

Whithan, G. B. 1973 *Linear and Nonlinear Waves*. Wiley.

Yih, C. S. 1965 *Dynamics of Nonhomogeneous Fluids*. Academic.

Yih, C. S. 1980 *Stratified Flows*. Academic.